

Efficient Semitransparent Organic Solar Cells with Tunable Color enabled by an Ultralow-Bandgap Nonfullerene Acceptor

Yong Cui, Chenyi Yang, Huifeng Yao,* Jie Zhu, Yuming Wang, Guoxiao Jia, Feng Gao, and Jianhui Hou*

Semitransparent organic solar cells (OSCs) show attractive potential in power-generating windows. However, the development of semitransparent OSCs is lagging behind opaque OSCs. Here, an ultralow-bandgap nonfullerene acceptor, "IEICO-4Cl", is designed and synthesized, whose absorption spectrum is mainly located in the near-infrared region. When IEICO-4Cl is blended with different polymer donors (J52, PBDB-T, and PTB7-Th), the colors of the blend films can be tuned from purple to blue to cyan, respectively. Traditional OSCs with a nontransparent Al electrode fabricated by J52:IEICO-4Cl, PBDB-T:IEICO-4Cl, and PTB7-Th:IEICO-4Cl yield power conversion efficiencies (PCE) of $9.65 \pm 0.33\%$, $9.43 \pm 0.13\%$, and $10.0 \pm 0.2\%$, respectively. By using 15 nm Au as the electrode, semitransparent OSCs based on these three blends also show PCEs of 6.37%, 6.24%, and 6.97% with high average visible transmittance (AVT) of 35.1%, 35.7%, and 33.5%, respectively. Furthermore, via changing the thickness of Au in the OSCs, the relationship between the transmittance and efficiency is studied in detail, and an impressive PCE of 8.38% with an AVT of 25.7% is obtained, which is an outstanding value in the semitransparent OSCs.

As a clean-energy technology, organic solar cells (OSCs)^[1–6] have attracted much attention from academia and industry due to their advantages in making large area panels by low-cost solution processing methods.^[7–10] Semitransparent OSCs that utilize transparent conductive electrodes and high-transmittance active layer materials show an attractive potential in power-generating windows.^[11–14] For the semitransparent OSCs, some critical requirements should be met: i) the power conversion efficiencies (PCEs) of the devices should be as high as possible and also the average visible transmittance (AVT, 370–740 nm)^[7]

of the devices should be good enough to fulfill the window applications;^[15] ii) The color of the semitransparent OSCs could be tuned to meet the requirements of varied applications.^[15–17]

Although the past two decades have seen much significant progress in OSCs, the development of semitransparent devices is relatively lagging behind because of the lack of suitable photoactive materials.^[8,18–21] Currently, the highly efficient OSCs with PCE over 11% were fabricated by the photoactive materials with optical absorption limited at around 800 nm.^[22–26] The strong absorption of the active materials in the visible range causes the great difficulty to make a balance between the PCE and transmittance, which is unfavorable for their application in semitransparent OSCs. For example, when a wide bandgap polymer donor PM6 and a fullerene derivative acceptor phenyl-C₇₁-butyric acid methyl ester (PC₇₁BM) were used to fabricate the semitransparent OSCs, the active layer thickness was only 75 nm. Although the device possessed high transparency, the inefficient light absorption resulted in its low short-circuit density (J_{SC}) of 9.4 mA cm⁻² and thus a moderate PCE of 5.7%, which was much lower than its opaque analog (9.2%).^[19] Semitransparent OSCs based on poly[[2,6'-4,8-di(5-ethylhexylthienyl)benzo[1,2-*b*:3,3-*b'*]dithiophene][3-fluoro-2[(2-ethylhexyl)carbonyl]thieno[3,4-*b'*]thiophenediyl]] (PTB7-Th):PC₇₁BM^[15] showed a high J_{SC} of 13.1 mA cm⁻² at 90–100 nm thickness, but its AVT was only

Y. Cui, C. Yang, Dr. H. Yao, J. Zhu, G. Jia, Prof. J. Hou
State Key Laboratory of Polymer Physics and Chemistry
Beijing National Laboratory for Molecular Sciences
CAS Research/Education Center for Excellence in Molecular Sciences
Institute of Chemistry
Chinese Academy of Sciences
Beijing 100190, China
E-mail: yaohf@iccas.ac.cn; hjhzl@iccas.ac.cn
Y. Cui, Prof. J. Hou
University of Chinese Academy of Sciences
Beijing 100049, China

C. Yang, G. Jia
School of Chemistry and Biology Engineering
University of Science and Technology Beijing
Beijing 100083, China
J. Zhu
Institute of Material Science and Engineering
Ocean University of China
Qingdao 266100, P. R. China
Y. Wang, Prof. F. Gao
Biomolecular and Organic Electronics IFM
Linköping University
Linköping 58183, Sweden

 The ORCID identification number(s) for the author(s) of this article can be found under <https://doi.org/10.1002/adma.201703080>.

DOI: 10.1002/adma.201703080

12.2%. In order to avoid strong absorption in the visible range and maintain relatively high absorption properties of the active layer, the main absorption peak of the photovoltaic material should be in the near-infrared (NIR) region, which is a feasible approach to achieve high PCE and high AVT simultaneously in semitransparent OSCs.

In OSCs using fullerene derivatives as acceptors, many low-bandgap donors with absorption spectra over 900 or even 1000 nm have been developed,^[27–31] whose absorption properties in the visible range are very weak. However, these studies suggested that this kind of OSC showed limited PCEs due to the large energy losses ($E_{\text{loss}} = E_{\text{g}}^{\text{opt}} - eV_{\text{OC}}$, where $E_{\text{g}}^{\text{opt}}$ is the optical bandgap of the active materials, and V_{OC} is the open-circuit voltage) and the low external quantum efficiency (EQE) in the NIR region.^[32,33] In the past few years, nonfullerene-based OSCs (NF-OSCs) have achieved many important progresses. Some results demonstrated that the absorption spectra of the NF acceptors could be extended to NIR region and the corresponding NF-OSCs exhibited high EQE and thus high PCE,^[21,34,35] offering a potential opportunity to promote the photovoltaic performance of semitransparent OSCs.

In this work, a novel NF acceptor, 2,2'-((2Z,2'Z)-(((4,4,9-tris(4-hexylphenyl)-9-(4-pentylphenyl)-4,9-dihydro-s-indaceno[1,2-*b*:5,6-*b*' dithiophene-2,7-diyl)bis(4-((2-ethylhexyl)oxy)thiophene-5,2-diyl))bis(methanylylidene))bis(5,6-dichloro-3-oxo-2,3-dihydro-1*H*-indene-2,1-diylidene))dimalononitrile (IEICO-4Cl), was designed and synthesized, which showed an ultralow bandgap ($E_{\text{g}}^{\text{opt}} = 1.23$ eV) and very weak absorption in the visible region (370–740 nm). When three polymers, poly[4-(4,8-bis(5-(2-ethylhexyl)thiophen-2-yl)benzo[1,2-*b*:4,5-*b*' dithiophen-2-yl)-5,6-difluoro-2-(2-hexyldecyl)-7-(thiophen-2-yl)-2*H*-benzo[*d*] [1,2,3]triazole] (J52), poly[(2,6-(4,8-bis(5-(2-ethylhexyl)thiophen-2-yl)benzo[1,2-*b*:4,5-*b*' dithiophene)-co-(1,3-di(5-thiophene-2-yl)-5,7-bis(2-ethylhexyl)benzo[1,2-*c*:4,5-*c*' dithiophene-4,8-dione)] (PBDB-T), and PTB7-Th with varied absorption properties were used as donors to blend with IEICO-4Cl, respectively, the colors of the blend films were determined by the polymers. In the

conventional OSCs with opaque Al as electrode, all the three devices based on these blends showed very good photovoltaic performance at low energy losses. Furthermore, photovoltaic performances of the semitransparent OSCs were fully investigated and the PTB7-Th:IEICO-4Cl-based OSCs yielded an impressive PCE of 8.38% with a high AVT of 25.7%.

For organic semiconductors, it has been demonstrated that the enhanced intramolecular charge transfer (ICT)^[36–38] from the electron-rich moiety to the electron-withdrawing groups can largely extend the absorption spectra of the resulting materials. Fluorination of the acceptor moiety has been proved to be an effective method to enhance the ICT effect.^[25,39,40] However, the fluorination procedure is generally tedious and costly, which is unfavorable for practical applications. In this contribution, as shown in the **Figure 1a**, we incorporate chlorination into the NF acceptor to enhance the ICT effect and thus redshifted its absorption spectrum. The detailed synthetic procedure of IEICO-4Cl is provided in the Supporting Information. IEICO-4Cl exhibits good solubility in common organic solvents, such as dichloromethane, chloroform, and chlorobenzene (CB). Thermogravimetric analysis suggests that IEICO-4Cl has good thermal stability with a decomposition temperature at ≈ 390 °C (Figure S1, Supporting Information).

The absorption spectra of IEICO-4Cl in diluted solution and as thin film are depicted in Figure 1c. In chloroform solution, IEICO-4Cl exhibits a maximum absorption peak at 802 nm, and the film has a redshift of 85 nm with an absorption onset of ≈ 1010 nm, corresponding to an $E_{\text{g}}^{\text{opt}}$ of 1.23 eV. It should be noted that the main absorption band of IEICO-4Cl film locates at 745–945 nm, which is out of the visible region and hence makes IEICO-4Cl a good candidate to fabricate semitransparent OSCs. Furthermore, when compared to 2,2'-((2Z,2'Z)-(((4,4,9-tris(4-hexylphenyl)-9-(4-pentylphenyl)-4,9-dihydro-s-indaceno[1,2-*b*:5,6-*b*' dithiophene-2,7-diyl)bis(4-((2-ethylhexyl)oxy)thiophene-5,2-diyl))bis(methanylylidene))bis(5,6-difluoro-3-oxo-2,3-dihydro-1*H*-indene-2,1-diylidene))dimalononitrile (IEICO-4F) in our recent work, IEICO-4Cl shows obviously

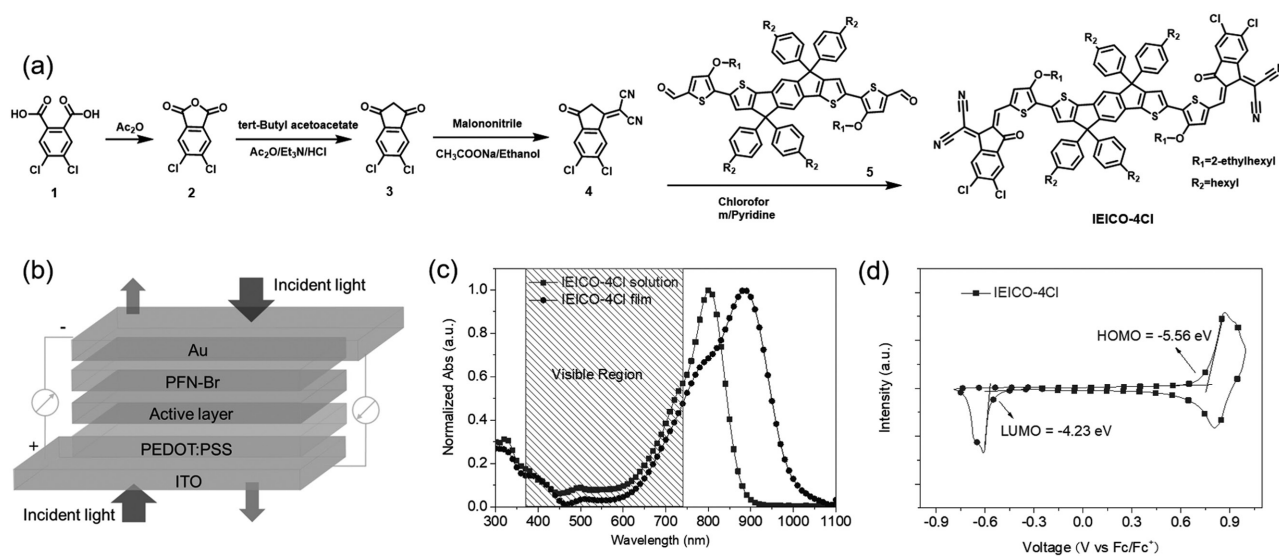


Figure 1. a) Synthetic routes of IEICO-4Cl. b) Device architecture of semitransparent OSCs in this work. c,d) Normalized absorption spectra (c) and CV curve (d) of IEICO-4Cl.

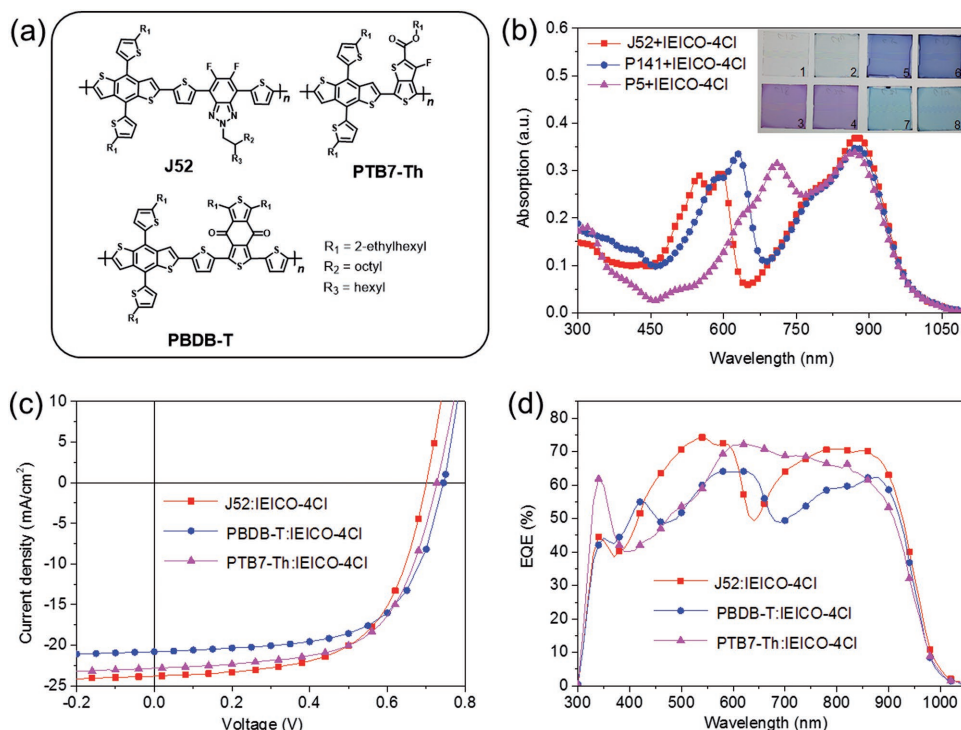


Figure 2. a) The molecular structure of J52, PBDB-T, and PTB7-Th. b) Absorption spectra of blend films. The inset is the photographs of blend and neat films. 1: ITO-Glass, 2: IEICO-4Cl, 3: J52, 4: J52:IEICO-4Cl, 5: PBDB-T, 6: PBDB-T:IEICO-4Cl, 7: PTB7-Th, 8: PTB7-Th:IEICO-4Cl. c,d) J - V curves (c) and EQE curves (d) of opaque OSCs based on J52:IEICO-4Cl, PBDB-T:IEICO-4Cl, and PTB7-Th:IEICO-4Cl.

redshifted absorption spectrum (Figure S2, Supporting Information),^[35] implying that chlorination is more effective than fluorination in enhancing the ICT effect. IEICO-4Cl is more suitable for utilizing NIR solar photons than IEICO-4F in the OSCs. As shown in Figure 1d, the molecular energy levels of IEICO-4Cl were measured by cyclic voltammetry (CV), and the highest occupied molecular orbital (HOMO) and the lowest unoccupied molecular orbital (LUMO) levels calculated from the onset of oxidation and reduction potentials are -5.56 and -4.23 eV, respectively.

The color of the blend active layer is determined by the absorption properties of both the donor and the acceptor. Since IEICO-4Cl has very weak absorption in the visible range, the colors of IEICO-4Cl-based blend films are highly dependent on the donors. Here, we selected three polymer donors named J52,^[41] PBDB-T,^[42] and PTB7-Th^[43] to blend with IEICO-4Cl (Figure 2a). As provided in Figure S3 (Supporting Information), the main absorption bands of the three polymers locate at 490–620, 530–660, and 620–745 nm, respectively, making their colors as purple, blue, and cyan. The blend films of J52:IEICO-4Cl, PBDB-T:IEICO-4Cl,

and PTB7-Th:IEICO-4Cl show very similar colors with the neat polymers (Figure 2b), demonstrating that the color of the blend film can be easily tuned by selecting different donors.

First, we investigated the photovoltaic characteristics of IEICO-4Cl via fabricating conventional opaque OSCs on indium tin oxide (ITO) substrate with Al as electrode, where the above-mentioned three polymers and poly(3,4-ethylenedioxythiophene)-polystyrenesulfonic acid (PEDOT:PSS)/poly[9,9-bis[6'-(N,N,N-trimethylammonium)hexyl]fluorene-alt-co-1,4-phenylene]-bromide (PFN-Br) were used as the donors and interlayers, respectively. After careful optimization of the device fabrication conditions like donor/acceptor ratios and solvent additives (Experimental Section), as shown in Figure 2c and Table 1, the OSCs based on J52:IEICO-4Cl, PBDB-T:IEICO-4Cl, and PTB7-Th:IEICO-4Cl show PCEs of $9.65 \pm 0.33\%$, $9.43 \pm 0.13\%$, and $10.0 \pm 0.2\%$, respectively, which are among the top values in the ultralow-bandgap OSCs.^[34,44,45] Specifically, the OSCs show similar V_{OC} around 0.72 V because of the similar HOMO levels (≈ -5.3 eV) for the three polymer donors, leading to very small energy losses around 0.5 eV (the calculated energy losses of

Table 1. The photovoltaic performance parameters of the conventional OSCs based on IEICO-4Cl.

| Donor | V_{OC} [V] | J_{SC} [mA cm ⁻²] | $J_{cal}^{a)}$ [mA cm ⁻²] | FF | PCE ^{b)} [%] | E_{loss} [eV] | Thickness [nm] |
|---------|-----------------|------------------------------------|--|-------|--------------------------|--------------------|-------------------|
| J52 | 0.700 | 23.8 | 23.3 | 0.607 | 10.1 (9.65 ± 0.33) | 0.530 | 110 |
| PBDB-T | 0.744 | 20.8 | 20.4 | 0.625 | 9.67 (9.43 ± 0.13) | 0.486 | 100 |
| PTB7-Th | 0.727 | 22.8 | 22.2 | 0.620 | 10.3 (10.0 ± 0.2) | 0.503 | 110 |

^{a)}Integrated J_{cal} from the EQE curves; ^{b)}The average parameters were calculated from more than ten independent cells.

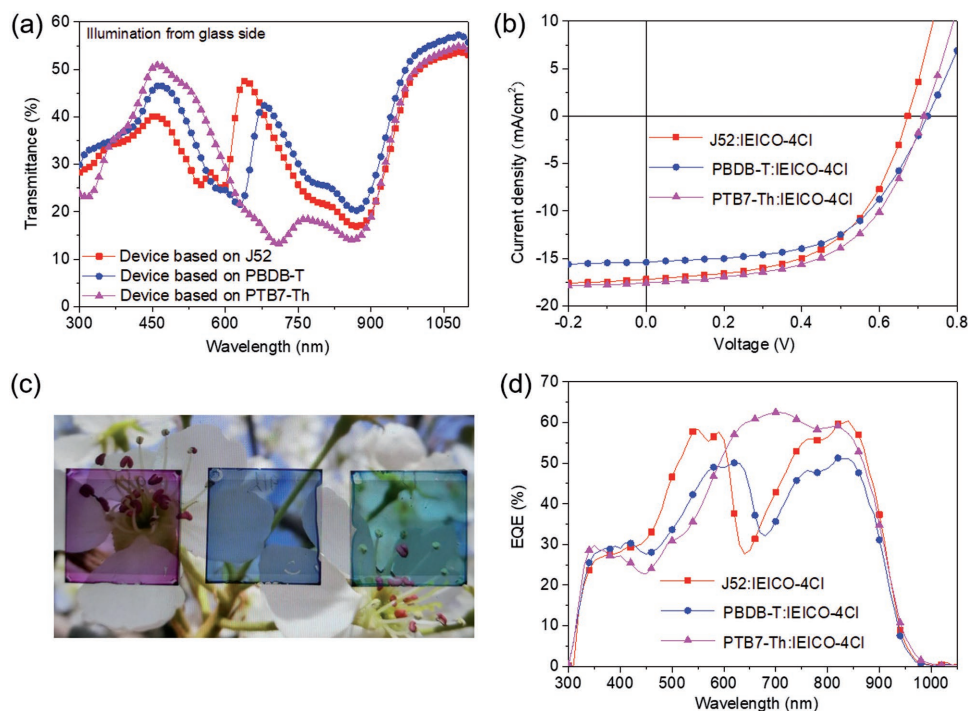


Figure 3. a,b) Transmission spectra (a) and J - V curves (b) of the semitransparent OSCs with Au (15 nm) illuminated from the ITO side. c) Photograph of the three semitransparent devices, from left to right are J52:IEICO-4Cl-, PBDB-T:IEICO-4Cl-, and PTB7-Th:IEICO-4Cl-based devices. d) EQE curves of the semitransparent OSCs.

the devices will be around 0.6 eV if the bandgap (E_g , 1.33 eV) of the blend is determined according to some reported literatures instead of E_g^{opt} (Figure S4, Supporting Information)^[46,47]. Impressively, all the three OSCs possess J_{SC} of over 20 mA cm⁻². When a transparent electrode is used in the OSCs, relatively high J_{SC} values are still guaranteed. Furthermore, the fill factors (FFs) of the three devices are all above 0.6.

The EQE spectra of the devices are displayed in Figure 2d, which are consistent with the absorption spectra of the corresponding blend films. All the three devices show high photoresponse in the whole absorption region, and the maximum EQE values of J52:IEICO-4Cl- and PTB7-Th:IEICO-4Cl-based devices are even over 70%, which are outstanding results for the OSCs with such low energy losses. The integrated current densities of the three OSCs from EQE spectra are 23.3, 20.4, and 22.2 mA cm⁻², respectively, which are in good agreement with those from the J - V measurements.

Via replacing Al with 15 nm Au as the transparent electrode in the devices, we fabricated the IEICO-4Cl-based semitransparent OSCs with a structure of ITO/PEDOT:PSS/active layers/PFN-Br/Au. **Figure 3a** shows the transmission spectra of the semitransparent devices, and the AVTs are 35.1%, 35.7%, and 33.5% for J52:IEICO-4Cl, PBDB-T:IEICO-4Cl, and PTB7-Th:IEICO-4Cl, respectively. From the optical photograph in **Figure 3c**, we can find that the colorful devices have very good transparency, and the background pattern can be clearly seen through the three semitransparent OSCs. **Figure 3b** shows the J - V curves of the devices, and the detailed photovoltaic parameters are collected in **Table 2**. Compared with their opaque devices, the V_{OC} and J_{SC} suffer some decreases, while the FF

increase a little in the semitransparent devices, and the resulting PCE values are 6.37%, 6.24%, and 6.97% for J52:IEICO-4Cl-, PBDB-T:IEICO-4Cl-, and PTB7-Th:IEICO-4Cl-based devices. The high PCEs along with its good transmittances of these devices make them very promising in the practical applications. The EQE curves of semitransparent devices are shown in **Figure 3d**. As Au has high transmittance in the range of 300–600 nm (**Figure S5**, Supporting Information), the EQE values have an obvious decrease in this range in comparison with that of the opaque devices. The integrated current densities from the EQE spectra are 16.1, 14.4, and 16.7 mA cm⁻² for J52:IEICO-4Cl-, PBDB-T:IEICO-4Cl-, and PTB7-Th:IEICO-4Cl-based semitransparent devices, respectively.

Since the 400–600 nm wavelength is the most sensitive region to human eyes,^[48] high transmittance is specially required in this region for the preparation of semitransparent OSCs. Among the three semitransparent OSCs, PTB7-Th:IEICO-4Cl has the highest average transmittance (AT, 400–600 nm) of 43.6% with a maximum transmittance of 50.9% at 462 nm, and its efficiency is the highest one. Therefore, we take PTB7-Th:IEICO-4Cl as an example to investigate the relationship of transmittance and efficiency of the semitransparent OSC by varying the thickness of Au. First, as shown in **Figure 4a**, as the thickness of Au increases from 10 to 30 nm, the AT of the devices decreases from 45.2% to 33.5% (the corresponding device pictures are provided in **Figure S6** in the Supporting Information). The increased thickness of Au contributes to the improved light reflection and lower series resistance in the devices, and hence, as shown in **Figure 4b** and **Table 2**, increased J_{SC} (16.8–19.6 mA cm⁻²) and FF (0.497–0.590) are

Table 2. The photovoltaic performance parameters of the semitransparent OSCs based on IEICO-4Cl.

| Active layer | Thickness of Au [nm] | Illumination ^{a)} | V_{OC} [V] | J_{SC} [mA cm^{-2}] | FF | PCE ^{b)} [%] | AVT [%] | AT [%] |
|-------------------|----------------------|----------------------------|--------------|----------------------------------|-------|-----------------------|---------|--------|
| J52:IEICO-4Cl | 15 | ITO | 0.673 | 17.2 | 0.551 | 6.37 (6.22 ± 0.12) | 35.1 | 33.1 |
| PBDB-T:IEICO-4Cl | 15 | ITO | 0.724 | 15.4 | 0.560 | 6.24 (6.04 ± 0.14) | 35.7 | 37.6 |
| PTB7-Th:IEICO-4Cl | 15 | ITO | 0.714 | 17.6 | 0.554 | 6.97 (6.76 ± 0.18) | 33.5 | 43.6 |
| PTB7-Th:IEICO-4Cl | 10 | ITO | 0.709 | 16.8 | 0.497 | 5.92 (5.51 ± 0.32) | 34.7 | 45.2 |
| PTB7-Th:IEICO-4Cl | 10 | Au | 0.700 | 11.4 | 0.501 | 4.00 (3.78 ± 0.15) | 34.5 | 45.1 |
| PTB7-Th:IEICO-4Cl | 15 | Au | 0.700 | 10.6 | 0.561 | 4.16 (4.01 ± 0.11) | 33.4 | 43.4 |
| PTB7-Th:IEICO-4Cl | 20 | ITO | 0.719 | 18.1 | 0.574 | 7.47 (7.24 ± 0.19) | 31.8 | 41.4 |
| PTB7-Th:IEICO-4Cl | 20 | Au | 0.695 | 9.49 | 0.587 | 3.87 (3.72 ± 0.13) | 31.7 | 41.3 |
| PTB7-Th:IEICO-4Cl | 25 | ITO | 0.722 | 18.8 | 0.583 | 7.91 (7.71 ± 0.17) | 28.2 | 36.8 |
| PTB7-Th:IEICO-4Cl | 25 | Au | 0.697 | 8.57 | 0.598 | 3.57 (3.46 ± 0.09) | 28.1 | 36.8 |
| PTB7-Th:IEICO-4Cl | 30 | ITO | 0.725 | 19.6 | 0.590 | 8.38 (8.17 ± 0.15) | 25.6 | 33.5 |
| PTB7-Th:IEICO-4Cl | 30 | Au | 0.699 | 7.36 | 0.617 | 3.17 (3.08 ± 0.06) | 25.7 | 33.6 |

^{a)}Semitransparent OSCs illuminated from the ITO or the Au side; ^{b)}The average parameters were calculated from more than ten independent cells.

obtained. Consequently, the PCE of the semitransparent device has a significant increase from 5.92% to 8.38%. To the best of our knowledge, the PCE of 8.38% with an AT of 33.5% (AVT of 25.6%) is one of the top values for semitransparent OSCs so far.

Furthermore, we investigated the photovoltaic performance of the PTB7-Th:IEICO-4Cl-based semitransparent OSC illuminated from Au electrode.^[49] The J - V characteristics are shown in Figure 4d and detailed photovoltaic parameters are collected in Table 2. With the increase of the thickness of Au, the J_{SC} of the corresponding devices decreases gradually due to the

absorption of Au. Compared with the photovoltaic performance of devices illuminated from the ITO side, the devices illuminated from the Au side show relatively lower V_{OC} and J_{SC} but higher FF. Consequently, the devices show an optimal PCE of 4.16%, with a V_{OC} of 0.70 V, a J_{SC} of 10.6 mA cm^{-2} , and a FF of 0.561 when 15 nm Au was used.

In summary, we have successfully designed and synthesized a new NF acceptor named IEICO-4Cl via chlorination, and its applications in efficient semitransparent OSCs were systematically studied. IEICO-4Cl has an ultralow bandgap of

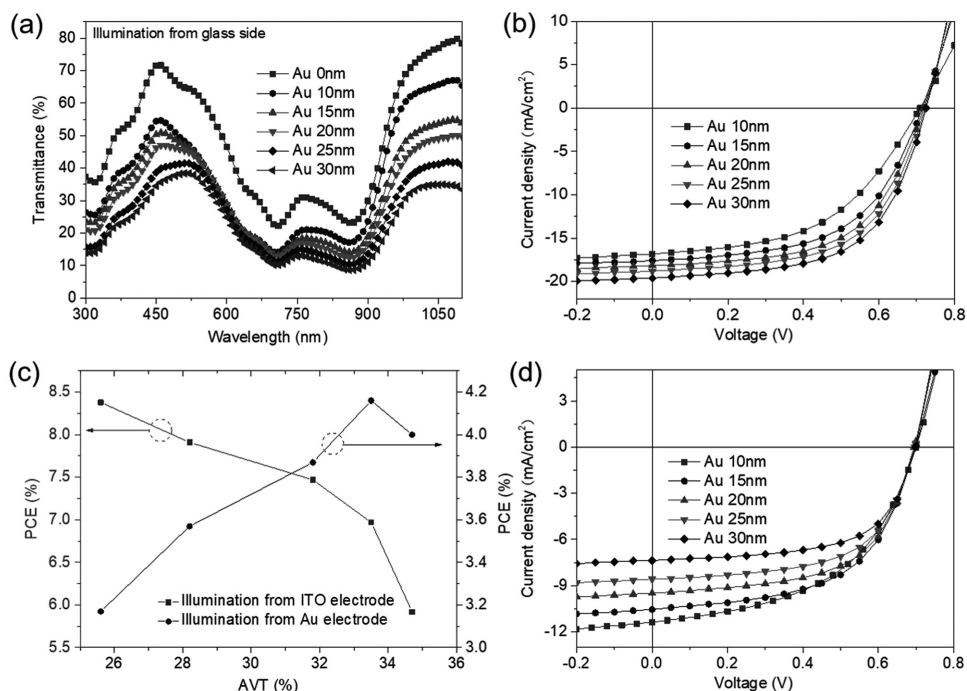


Figure 4. a,b) Transmission spectra (a) and J - V curves (b) of the semitransparent OSCs based on PTB7-Th with different Au thickness illuminated from the ITO side. c) Relationships between the PCE and the transmittance of the semitransparent OSCs illuminated from the ITO and the Au sides. d) J - V curves of the semitransparent OSCs based on PTB7-Th with different thicknesses of Au illuminated from the Au side.

1.23 eV with weak absorption in the visible region. The colors of IEICO-4Cl-based blend films could be easily tuned from purple, blue to cyan via selecting J52, PBDB-T, and PTB7-Th as polymer donors, respectively. In the conventional opaque OSCs with Al electrode, PCE around 10% with a low E_{loss} of 0.5 eV was recorded. Furthermore, the semitransparent OSCs were fabricated by using 15 nm Au as electrode, and J52:IEICO-4Cl-, PBDB-T:IEICO-4Cl-, and PTB7-Th:IEICO-4Cl-based devices yielded high PCE of 6.37%, 6.24%, and 6.97% with high AVT of 35.1%, 35.7%, and 33.5%, respectively. Furthermore, via changing the thickness of Au in the OSCs, the relationship between the transmittance and efficiency was studied in detail, and an impressive PCE of 8.38% with an AVT of 25.6% was obtained, which is an outstanding value in the semitransparent OSCs. These results demonstrate that design and application of ultralow-bandgap NF acceptor is an effective strategy to improve the photovoltaic performance of semitransparent OSCs.

Experimental Section

Solar-Cell Fabrication: All devices were fabricated with the conventional structure of glass/ITO/PEDOT:PSS/active layers/PFN-Br/Al or Au. First, PEDOT:PSS (Clevios P VP Al. 4083) was diluted with the same volume of water, and then the preprocessed PEDOT:PSS was spin coated on the precleaned ITO substrates and annealed at 150 °C for 20 min. Active layer solutions were prepared with the following methods. PBDB-T and IEICO-4Cl were mixed at a ratio of 1:1, while other polymer donors and IEICO-4Cl were mixed at a ratio of 1:1.5. Active layer materials were fully dissolved in CB at a polymer concentration of 10 mg mL⁻¹ and the solution was stirred for at least 2 h. Before spin coating, 1% volume of 1,8-iodooctane was added to the solution of J52:IEICO-4Cl and PBDB-T:IEICO-4Cl, respectively. Then, the active layer was spin coated on the PEDOT:PSS and all the films were heated at 100 °C for 10 min. About 2 nm PFN-Br (dissolved in methanol with the concentration of 0.5 mg mL⁻¹) layer was spin-coated on the top of all the active layers. Finally, Al or Au layer was deposited under high vacuum ($\approx 3 \times 10^{-4}$ Pa).

Device Characterization and Measurement: *J*-*V* characteristics of the devices were measured by using a AAA solar simulator (XES-70S1, SAN-EI Electric Co., Ltd.) with 100 mW cm⁻². Before each test, the solar simulator was calibrated with a standard Si solar cell (made by Enli Technology Co., Ltd., Taiwan, calibrated by the NMI). The EQE was measured through the Solar Cell Spectral Response Measurement System QE-R3011 (Enli Technology Co., Ltd., Taiwan).

Supporting Information

Supporting Information is available from the Wiley Online Library or from the author.

Acknowledgements

The authors would like to acknowledge the financial support from the National Natural Science Foundation of China (91633301, 51673201, 91333204, 21325419) and the Chinese Academy of Sciences (XDB12030200).

Conflict of Interest

The authors declare no conflict of interest.

Keywords

nonfullerene acceptors, organic solar cells, semitransparent, tunable color

Received: June 1, 2017

Revised: August 3, 2017

Published online:

- [1] A. J. Heeger, *Adv. Mater.* **2014**, *26*, 10.
- [2] F. C. Krebs, *Sol. Energy Mater. Sol. Cells* **2009**, *93*, 394.
- [3] C. J. Brabec, *Sol. Energy Mater. Sol. Cells* **2004**, *83*, 273.
- [4] G. Yu, J. Gao, J. C. Hummelen, F. Wudl, A. J. Heeger, *Science* **1995**, *270*, 1789.
- [5] R. Søndergaard, M. Hösel, D. Angmo, T. T. Larsen-Olsen, F. C. Krebs, *Mater. Today* **2012**, *15*, 36.
- [6] M. Kaltenbrunner, M. S. White, E. D. Glowacki, T. Sekitani, T. Someya, N. S. Sariciftci, S. Bauer, *Nat. Commun.* **2012**, *3*, 770.
- [7] K.-S. Chen, J.-F. Salinas, H.-L. Yip, L. Huo, J. Hou, A. K. Y. Jen, *Energy Environ. Sci.* **2012**, *5*, 9551.
- [8] Z. M. Beiley, M. G. Christoforo, P. Gratia, A. R. Bowring, P. Eberspacher, G. Y. Margulis, C. Cabanetos, P. M. Beaujuge, A. Salleo, M. D. McGehee, *Adv. Mater.* **2013**, *25*, 7020.
- [9] Y. Wang, B. Jia, F. Qin, Y. Wu, W. Meng, S. Dai, Y. Zhou, X. Zhan, *Polymer* **2016**, *107*, 108.
- [10] C.-C. Chen, L. Dou, J. Gao, W.-H. Chang, G. Li, Y. Yang, *Energy Environ. Sci.* **2013**, *6*, 2714.
- [11] F. Pastorelli, P. Romero-Gomez, R. Betancur, A. Martinez-Otero, P. Mantilla-Perez, N. Bonod, J. Martorell, *Adv. Energy Mater.* **2015**, *5*, 1400614.
- [12] F. Guo, S. Chen, Z. Chen, H. Luo, Y. Gao, T. Przybilla, E. Spiecker, A. Osvet, K. Forberich, C. J. Brabec, *Adv. Opt. Mater.* **2015**, *3*, 1524.
- [13] J. Y. Lee, S. T. Connor, Y. Cui, P. Peumans, *Nano Lett.* **2010**, *10*, 1276.
- [14] B. Norton, P. C. Eames, T. K. Mallick, M. J. Huang, S. J. McCormack, J. D. Mondol, Y. G. Yohanis, *Sol. Energy* **2011**, *85*, 1629.
- [15] G. Xu, L. Shen, C. Cui, S. Wen, R. Xue, W. Chen, H. Chen, J. Zhang, H. Li, Y. Li, Y. Li, *Adv. Funct. Mater.* **2017**, *27*, 1605908.
- [16] A. Colmann, A. Puetz, A. Bauer, J. Hanisch, E. Ahlswede, U. Lemmer, *Adv. Energy Mater.* **2011**, *1*, 599.
- [17] T. Ameri, G. Dennler, C. Waldauf, H. Azimi, A. Seemann, K. Forberich, J. Hauch, M. Scharber, K. Hingerl, C. J. Brabec, *Adv. Funct. Mater.* **2010**, *20*, 1592.
- [18] C.-Y. Chang, L. Zuo, H.-L. Yip, Y. Li, C.-Z. Li, C.-S. Hsu, Y.-J. Cheng, H. Chen, A. K. Y. Jen, *Adv. Funct. Mater.* **2013**, *23*, 5084.
- [19] M. Zhang, X. Guo, W. Ma, H. Ade, J. Hou, *Adv. Mater.* **2015**, *27*, 4655.
- [20] C. C. Chen, L. T. Dou, R. Zhu, C. H. Chung, T. B. Song, Y. B. Zheng, S. Hawks, G. Li, P. S. Weiss, Y. Yang, *ACS Nano* **2012**, *6*, 7185.
- [21] F. Liu, Z. Zhou, C. Zhang, J. Zhang, Q. Hu, T. Vergote, F. Liu, T. P. Russell, X. Zhu, *Adv. Mater.* **2017**, *29*, 1606574.
- [22] W. Zhao, S. Li, H. Yao, S. Zhang, Y. Zhang, B. Yang, J. Hou, *J. Am. Chem. Soc.* **2017**, *139*, 7148.
- [23] S. Li, L. Ye, W. Zhao, S. Zhang, S. Mukherjee, H. Ade, J. Hou, *Adv. Mater.* **2016**, *28*, 9423.
- [24] J. Zhao, Y. Li, G. Yang, K. Jiang, H. Lin, H. Ade, W. Ma, H. Yan, *Nat. Energy* **2016**, *1*, 15027.
- [25] F. Zhao, S. Dai, Y. Wu, Q. Zhang, J. Wang, L. Jiang, Q. Ling, Z. Wei, W. Ma, W. You, C. Wang, X. Zhan, *Adv. Mater.* **2017**, *29*, 1700144.
- [26] H. Yao, J. Hou, *Acta Polym. Sin.* **2016**, *11*, 1468.
- [27] H. Bronstein, E. Collado-Fregoso, A. Hadipour, Y. W. Soon, Z. Huang, S. D. Dimitrov, R. S. Ashraf, B. P. Rand, S. E. Watkins,

- P. S. Tuladhar, I. Meager, J. R. Durrant, I. McCulloch, *Adv. Funct. Mater.* **2013**, *23*, 5647.
- [28] J. C. Bijleveld, R. A. M. Verstrijden, M. M. Wienk, R. A. J. Janssen, *J. Mater. Chem.* **2011**, *21*, 9224.
- [29] I. Meager, R. S. Ashraf, S. Mollinger, B. C. Schroeder, H. Bronstein, D. Beatrup, M. S. Vezie, T. Kirchartz, A. Salleo, J. Nelson, I. McCulloch, *J. Am. Chem. Soc.* **2013**, *135*, 11537.
- [30] E. Zhou, J. Cong, K. Hashimoto, K. Tajima, *Energy Environ. Sci.* **2012**, *5*, 9756.
- [31] K. H. Hendriks, W. Li, M. M. Wienk, R. A. Janssen, *J. Am. Chem. Soc.* **2014**, *136*, 12130.
- [32] K. Kawashima, Y. Tamai, H. Ohkita, I. Osaka, K. Takimiya, *Nat. Commun.* **2015**, *6*, 10085.
- [33] W. W. Li, K. H. Hendriks, A. Furlan, M. M. Wienk, R. A. J. Janssen, *J. Am. Chem. Soc.* **2015**, *137*, 2231.
- [34] H. Yao, Y. Chen, Y. Qin, R. Yu, Y. Cui, B. Yang, S. Li, K. Zhang, J. Hou, *Adv. Mater.* **2016**, *28*, 8283.
- [35] H. Yao, Y. Cui, R. Yu, B. Gao, H. Zhang, J. Hou, *Angew. Chem., Int. Ed.* **2017**, *56*, 3045.
- [36] Y. Lin, Z. G. Zhang, H. Bai, Y. Li, X. Zhan, *Chem. Commun.* **2012**, *48*, 9655.
- [37] J. Roncali, *Chem. Rev.* **1997**, *97*, 173.
- [38] S. Zeng, L. Yin, C. Ji, X. Jiang, K. Li, Y. Li, Y. Wang, *Chem. Commun.* **2012**, *48*, 10627.
- [39] T. L. Nguyen, H. Choi, S. J. Ko, M. A. Uddin, B. Walker, S. Yum, J. E. Jeong, M. H. Yun, T. J. Shin, S. Hwang, J. Y. Kim, H. Y. Woo, *Energy Environ. Sci.* **2014**, *7*, 3040.
- [40] D. Deng, Y. Zhang, J. Zhang, Z. Wang, L. Zhu, J. Fang, B. Xia, Z. Wang, K. Lu, W. Ma, Z. Wei, *Nat. Commun.* **2016**, *7*, 13740.
- [41] H. Bin, Z. G. Zhang, L. Gao, S. Chen, L. Zhong, L. Xue, C. Yang, Y. Li, *J. Am. Chem. Soc.* **2016**, *138*, 4657.
- [42] D. Qian, L. Ye, M. Zhang, Y. Liang, L. Li, Y. Huang, X. Guo, S. Zhang, Z. A. Tan, J. Hou, *Macromolecules* **2012**, *45*, 9611.
- [43] S. H. Liao, H. J. Jhuo, Y. S. Cheng, S. A. Chen, *Adv. Mater.* **2013**, *25*, 4766.
- [44] Y. Jin, Z. Chen, S. Dong, N. Zheng, L. Ying, X. F. Jiang, F. Liu, F. Huang, Y. Cao, *Adv. Mater.* **2016**, *28*, 9811.
- [45] H. Choi, S. J. Ko, T. Kim, P. O. Morin, B. Walker, B. H. Lee, M. Leclerc, J. Y. Kim, A. J. Heeger, *Adv. Mater.* **2015**, *27*, 3318.
- [46] J. Liu, S. Chen, D. Qian, B. Gautam, G. Yang, J. Zhao, J. Bergqvist, F. Zhang, W. Ma, H. Ade, O. Inganäs, K. Gundogdu, F. Gao, H. Yan, *Nat. Energy* **2016**, *1*, 16089.
- [47] E. T. Hoke, K. Vandewal, J. A. Bartelt, W. R. Mateker, J. D. Douglas, R. Noriega, K. R. Graham, J. M. J. Fréchet, A. Salleo, M. D. McGehee, *Adv. Energy Mater.* **2013**, *3*, 220.
- [48] H. Morkoc, S. N. Mohammad, *Science* **1995**, *267*, 51.
- [49] C. Tao, G. Xie, C. Liu, X. Zhang, W. Dong, F. Meng, X. Kong, L. Shen, S. Ruan, W. Chen, *Appl. Phys. Lett.* **2009**, *95*, 053303.